Statistical Theory of Nuclear Fission: Asymmetric Fission*

PETER FONG†
Institute for Nuclear Studies, University of Chicago, Chicago, Illinois
(Received October 28, 1955)

A statistical theory is developed, according to which the relative probability of a mode of fission is determined by the total excitation energy of its two fragments calculated at the moment just before separation. In order to calculate the excitation energy, the well known semiempirical atomic mass formula is corrected for its deviations known to be attributed to the effects of nuclear shells. The nuclear level density expression is studied empirically with special attention to shell effects. These results are used for a quantitative calculation of the relative probabilities of all possible modes of fission. The mass distribution curve of fission products of U^{235} induced by thermal neutrons is derived and compared with experimental results. Applications of the statistical theory to charge distribution, kinetic energy distribution, variations of mass, charge and energy distributions with respect to target nucleus and incident energy, prompt neutron distribution, spontaneous fission yields, and ternary fission will be discussed briefly.

I. INTRODUCTION

THE problem of asymmetric fission has been discussed by many authors.[1] However, there is no quantitative calculation leading to a derivation of the double-humped mass distribution curve of the fission products.[2] Also there is no unified interpretation of many diversified fission characteristics.[3]

Calculations of atomic masses by Bohr and Wheeler[4] and by Frankel and Metropolis,[5] based on the liquid drop model, (L.D.M.) give the result that the *total energy release* is largest for symmetric fission. The L.D.M. mass formula (by which we mean the formula given by Fermi[6] and used by Metropolis and Reitwiesner to calculate their mass table[7] sometimes disagrees markedly with experiment. Recent progress on determination of nuclear masses (Sec. II) enables us to calculate the total energy release more accurately. This calculation shows that the total energy release of some asymmetric modes of fission may be larger than that of symmetric fission by 2 Mev (Sec. II). As the total energy release is of the order of 200 Mev, the difference of 1% at first seems to be insignificant. However, most of the energy released is derived from the Coulomb potential between the two fragments. The internal excitation energy, a small portion of the 200-Mev total, is estimated by Brunton[8] to be of the order of only 20 Mev. As the Coulomb energy is largest for symmetric fission (Sec. IV), the difference in excitation energy between asymmetric and symmetric modes will be even larger. It will be shown (Sec. VI) that the energy of internal excitation of the fission products with a mass ratio of about 1.5 is greater than that of symmetrical fission by about 5 Mev. Recent experiments on neutron distribution also support this fact (Sec. VI). The difference of 5 Mev out of about 20 Mev is no longer insignificant. Frankel and Metropolis[5] calculated the shape of the fissioning nucleus at the saddle point of the energy on the basis of the Bohr-Wheeler formula. They found that this shape is symmetric, but does not show a "neck" at which the deformed nucleus might break. The calculation by Hill[9] demonstrates that the fission process is slow enough so that the surface waves travel from one end to the other many times before a definite neck develops and fission occurs. It can also be estimated that the process from saddle point to separation is sufficiently slow for a nucleon to cross the nucleus many times. Therefore, it is possible that the fission modes will be determined at a rather late stage, probably just before the separation of the fragments. Furthermore, because of the slowness of the fission process, we may assume that an instantaneous statistical equilibrium will be established at any instant of the process, from saddle point to separation. According to this assumption, any relative probability of

* This paper is based on a Ph.D. thesis submitted to the Department of Physics, University of Chicago, December, 1953. Preliminary results have been published in a Letter to the Editor [Peter Fong, Phys. Rev. **89**, 332 (1953)].

† Now at Department of Physics, Utica College of Syracuse University, Utica, New York.

[1] R. D. Present and J. K. Knipp, Phys. Rev. **57**, 751 (1940); J. Frenkel, J. Phys. (U.S.S.R.) **10**, 533 (1946); A. J. Dempster, Phys. Rev. **72**, 431 (1947); S. Frankel and N. Metropolis, Phys. Rev. **72**, 914 (1947); P. F. Gast, Phys. Rev. **72**, 1265 (1947); E. Bagge, Z. Naturforsch. **2a**, 565 (1947); M. G. Mayer, Phys. Rev. **74**, 235 (1948); K. H. Kingdom, Phys. Rev. **76**, 136 (1949); G. C. Wick, Phys. Rev. **76**, 181 (1949); L. Meitner, Nature **165**, 561 (1950) and Arkiv Fysik **4**, 383 (1952); T. Yasaki and O. Miyatake, Phys. Rev. **79**, 740 (1950); and **80**, 754 (1950); O. Miyatake, Progr. Theoret. Phys. **7**, 285 (1952); D. L. Hill, Phys. Rev. **78**, 330 (1950) and **79**, 197 (1951); J. Jungerman, Phys. Rev. **80**, 285 (1950); J. A. Wheeler and D. L. Hill, Phys. Rev. **83**, 236(A) (1951); H. G. Thode, Trans. Roy. Soc. Canada **45**, 1 (1951); W. J. Swiatecki, Phys. Rev. **83**, 178 (1951); T. D. Newton, Phys. Rev. **87**, 187 (1952); D. L. Hill and J. A. Wheeler, Phys. Rev. **89**, 1102 (1953).

[2] C. D. Coryell and N. Sugarman, Editors, *Radiochemical Studies: The Fission Products* (McGraw-Hill Book Company, Inc., New York, 1951), National Nuclear Energy Series, Plutonium Project Record, Vol. 9; The Plutonium Project, Revs. Modern Phys. **18**, 513 (1946) or J. Am. Chem. Soc. **68**, 2411 (1946).

[3] See review article by W. J. Whitehouse, Progr. Nuclear Phys. **2**, 120 (1952).

[4] N. Bohr and J. A. Wheeler, Phys. Rev. **56**, 426 (1939).

[5] S. Frankel and N. Metropolis, Phys. Rev. **72**, 914 (1947).

[6] E. Fermi, *Nuclear Physics Notes* (University of Chicago Press, Chicago, 1949), pp. 6–8.

[7] N. Metropolis and G. Reitwiesner, U. S. Atomic Energy Commission Report NP–1980, 1950 (unpublished).

[8] D. C. Brunton, Phys. Rev. **76**, 1798 (1949).

[9] D. L. Hill, Phys. Rev. **79**, 197 (1950).

occurrence is proportional to the corresponding density of quantum states. The observed relative probabilities of fission modes are thus proportional to densities of quantum states of the corresponding nuclear configurations at the moment when statistical equilibrium is last established, presumably the moment just before separation. For convenience of calculation we approximate the configuration at this *critical moment* by that of two deformed fragments in contact. The density of quantum states of this configuration may be calculated; its value obviously depends on the excitation energies of the two fragments at this critical moment. Larger excitation energy corresponds to larger density of quantum states and thus to larger relative probability. The density of excitation states of a nucleus, usually expressed by an exponential function, $c\exp[2(aE)^{\frac{1}{2}}]$, is a rapidly increasing function of the excitation energy (Sec. III). A small change in excitation energy may thus result in a large change of the relative probability. That asymmetric fission has an excitation energy larger than symmetric fission by 5 Mev leads to a larger relative probability for asymmetric fission. In this paper the density of quantum states at the critical moment will be calculated (Sec. V). This quantity turns out to be a function of the mass numbers, charge numbers and Coulomb energy of the two fragments, and depends parametrically on the target nucleus, incident particle, and bombarding energy. This enables us to derive quantitatively the mass distribution, charge distribution, kinetic energy distribution and many other distributions of the fission products, as well as the parametric dependence of these distributions on target nucleus, incident particle and bombarding energy. The asymmetry in mass splitting will be discussed in detail (Sec. VI). Other applications will be discussed briefly (Sec. VII) and their details will be published in the future.

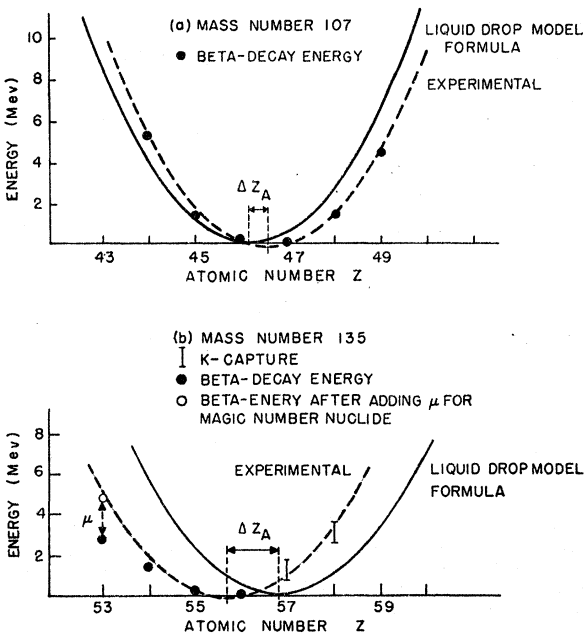

FIG. 1. Energy of isobars. (a) Mass number 107. (b) Mass number 135.

II. ATOMIC MASSES IN THE FISSION-PRODUCT REGION

Since the primary fission products are short-lived, there are no direct measurements of their masses. The mass determination has to rely on indirect methods.

Calculation of atomic masses usually starts with a semiempirical mass formula based on the liquid-drop model of the nucleus.[10] This formula can be written as follows:

$$M(A,Z)=M_A+B_A(Z-Z_A)^2+\delta_A. \tag{1}$$

The first term corresponds to the mass of the beta-stable nucleus. The second term corresponds to the beta-decay energy. The last term is the even-odd energy. The constants in Eq. (1), determined by Fermi,[6] are as follows (all in amu):

$$\begin{aligned} M_A&=1.01464A+0.014A^{\frac{2}{3}}-0.041905Z_A,\\ B_A&=0.041905/Z_A,\\ Z_A&=A/(1.980670+0.0149624A^{\frac{2}{3}}),\\ \delta_A&=\frac{0.036}{A^{3/4}}\times\begin{cases}1 & \text{odd-odd}\\ 0 & \text{odd-}A\\ -1 & \text{even-even.}\end{cases}\end{aligned} \tag{2}$$

This set of parameters has been used by Metropolis and Reitwiesner[7] in an elaborate tabulation of atomic masses which is widely used.

This mass formula represents the atomic masses fairly well for a wide range of mass numbers. However, recent measurements of atomic masses show that local deviations from this formula of the order of 10 Mev exist. If an accuracy of a few Mev is important these deviations have to be corrected. The first term M_A of Eq. (1) may be compared with the experimental masses of stable nuclei. The second term may be compared with the experimental beta-decay energies. Thus corrections to M_A, B_A, and Z_A may be obtained (δ_A is assumed to be correct). It is a common practice to assume M_A, B_A, and Z_A to be continuous functions of the mass number A and to determine them by extrapolating known experimental values.

We use the experimentally known beta-decay energies[11] to plot the empirical energy differences of isobaric nuclides. These curves may be compared with those determined from Eqs. (1) and (2). A comparison of these isobaric curves for two mass numbers is shown in Fig. 1 as an example. The Z_A correction ΔZ_A may be

[10] C. D. Coryell, Ann. Rev. Nuc. Sci. **2**, 305 (1953). This paper gives a comprehensive review of expressions of atomic masses.

[11] Way, Fano, Scott, and Thew, *Nuclear Data*, National Bureau of Standards Circular No. 499 (U. S. Government Printing Office, Washington, D. C., 1950), and Supplements. These summarize all experimental results of beta-decay energies.

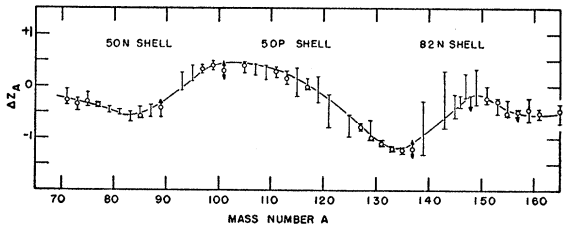

FIG. 2. Correction curve for liquid-drop model values of the most stable charge Z_A. $\Delta Z_A = Z_A$ (experimental) $- Z_A$ (liquid-drop model).

found directly by comparing the positions of the bottoms of the two curves. The B_A value may be checked by comparing the curvatures of these two curves. This procedure has been applied to isobaric nuclides of nearly all odd mass numbers between 71 and 165 (fission-product region). The odd mass numbers are used to avoid the even-odd complication. When no magic number is involved, the parabolic approximation is generally good, as can be seen in Fig. 1. No noticeable deviation of curvature is found. Thus we assume the B_A values given by Eq. (2) to be correct. On the other hand, the Z_A values given by Eq. (2) deviate from the actual values considerably. The deviation may be either positive or negative, as can be seen in Fig. 1, with a maximum of the order of one charge unit. The ΔZ_A values, defined as $Z_A(\text{exp}) - Z_A(\text{L.D.M.})$, for odd mass numbers between 71 and 165, are plotted in Fig. 2 with their estimated errors. When the determination is uncertain only limits are given. A smooth curve may be drawn as the correction curve of Z_A. To determine M_A, we compare the values obtained from Eqs. (1) and (2) with the mass-spectroscopically determined masses of stable isotopes. The data used are those of Duckworth *et al.*[12] and of Halsted.[13] Since a stable isotope is usually not situated at the bottom of the isobaric parabola, a small correction has to be applied to bring the experimental mass value to that at the bottom of the parabola. (For odd-A stable nuclides, Z differs from Z_A by less than 0.5 unit and this correction is usually less than 0.3 Mev.) The correction ΔM_A, defined as $M_A(\text{exp}) - M_A(\text{L.D.M.})$, is plotted in Fig. 3 for those isotopes whose masses are known experimentally. A smooth curve may be drawn as the M_A correction curve. The curve passes through most of the points except the magic number nuclides. In the following we will discuss the magic number effects.

The assumption of continuous values of M_A, B_A, and Z_A has been used many times before. It is a good approximation except for cases where magic-number nuclides are involved. Therefore, it has to be modified in order to include the magic nuclides. Experimental evidence indicates that a discontinuity exists at the magic numbers. For example, the points corresponding to Sn^{116} and Sn^{124} (50 protons) in Fig. 3 are lower than the nonmagic ones of the same mass by about 1 Mev. That magic number nuclides are more tightly bound than others can be observed also from the abrupt change in the neutron binding energies of the order of 2 Mev at the shell edges.[14] These suggest that a discontinuous term μ, analogous to the δ_A term, may be introduced in Eq. (1) to account for the discontinuous variation of nuclear binding energy at shell edges. μ will be between -1 and -2 Mev for magic nuclides and zero for others. From Fig. 3 the value of μ (50 protons) may be estimated to be about -1.1 Mev. From the difference in neutron binding energies,[14] the values of μ (50 neutrons) and μ (82 neutrons) are estimated to be both -2.0 Mev. As the discontinuities at magic numbers are attributed to the μ term, the mass values after removing the μ term are expected to vary continuously. In Fig. 3 the masses of magic nuclides, after removing the μ term, are also given. A continuous smooth curve may now be drawn through these points and the nonmagic nuclides.

The isobaric curves involving a magic-number nuclide are usually not a smooth parabola, as can be seen in Fig. 1(b). If the mass of the magic nuclide is corrected for the μ term, it fits the parabola better. Thus the introduction of μ seems to be able to account for the irregularities associated with magic numbers. Our correction curves ΔZ_A and ΔM_A are both obtained from mass data after removing μ. Thus they may be represented by continuous curves.

In summary we may express the corrected mass formula (in the fission-product region) as follows:

$$M(A,Z) = M_A + \Delta M_A + B_A(Z - Z_A - \Delta Z_A)^2 + \delta_A + \mu, \quad (3)$$

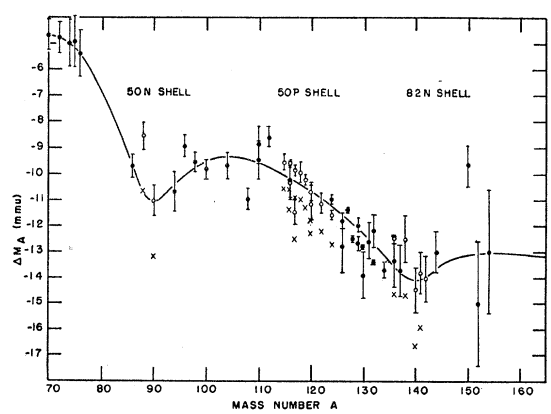

FIG. 3. Correction curve for liquid-drop-model values of the mass of stable isobar M_A. $\Delta M_A = M_A$ (experimental) $- M_A$ (liquid drop model). The symbols ●, ×, and ○ represent the nonmagic-number nuclides, magic-number nuclides and magic-number nuclides after adding μ, respectively.

[12] Duckworth, Kegley, Olson, and Stanford, Phys. Rev. **83**, 1114 (1951); H. E. Duckworth, (unpublished, 1952); H. E. Duckworth and R. S. Preston, Phys. Rev. **82**, 468 (1951); H. E. Duckworth, Nature **170**, 158 (1952).

[13] R. E. Halsted, Phys. Rev. **85**, 726 (1952); **88**, 666 (1952).

[14] M. G. Mayer, Phys. Rev. **74**, 235 (1948); J. A. Harvey, Phys. Rev. **81**, 353 (1951); H. E. Suess, Phys. Rev. **81**, 1071 (1951); H. E. Suess and J. H. D. Jensen, Arkiv Fysik **3**, 577 (1951).

TABLE I. Comparison of Z_A values of the General Electric Company chart of nuclides and this paper.

Mass number	75	85	95	105	115	125	135	145	155	165
Z_A (G.E. chart)	33.15	36.89	41.88	45.82	49.73	52.24	55.61	60.41	63.71	67.29
Z_A (this paper)	33.06	36.91	41.58	45.82	49.40	52.54	55.67	60.16	63.80	67.34

where M_A, B_A, Z_A, and δ_A are given by Eq. (2), ΔM_A and ΔZ_A are given by Fig. 2 and Fig. 3, respectively and μ is given by

$$\begin{aligned} \mu\ (50\text{ neutrons}) &= -2.0\text{ Mev}, \\ \mu\ (82\text{ neutrons}) &= -2.0\text{ Mev}, \\ \mu\ (50\text{ protons}) &= -1.1\text{ Mev}, \\ \mu = 0 &\text{ for nonmagic-number nuclides.} \end{aligned} \tag{4}$$

This formula differs from Eq. (1) by the inclusion of ΔM_A, ΔZ_A, and μ. The μ term is directly related to the magic numbers. The ΔM_A and ΔZ_A terms are also influenced by the nuclear shells. The dips of the ΔM_A curve in Fig. 3 are found at the regions of 50 and 82 neutrons. (These indicate that nuclear masses are generally lower by a few Mev in the broad neighborhood of shell edges and reach minimum at magic numbers.) ΔZ_A remains nearly constant in the shell-free regions but increases when a neutron shell is filling and decreases when a proton shell is filling. As the correction terms reflect the shell effects, this formula may be regarded as the liquid-drop model formula corrected for the shell effects.

During the progress of this work many papers have been published discussing the shell effects on nuclear masses. Coryell *et al.*[15,10] introduced discontinuous Z_A values to account for the shell effects. Wapstra[16] discussed the changes of the beta-stability line near closed nuclear shells. Nier *et al.*[17,13] used Wigner's mass formula and determined its parameters empirically for different regions between the shells. Green *et al.*[18] also gave empirical corrections of the liquid-drop model mass formula. The general attitude is to introduce some new term or some discontinuous parameters to account for the abrupt changes at shell edges.

Empirical determination of the beta-stability line Z_A has been made by Bohr and Wheeler,[4] Way,[19] Joliot-Curie,[20] Feenberg,[21] Kohman,[22] Sullivan[23] and Stehn.[24] Many of them assumed that the beta-stability line passes within 0.5 charge unit through the charge numbers of stable nuclei. The Z_A values given by the General Electric Company Chart of Nuclides[24] are compared with the present values in Table I.

The corrected mass formula, Eq. (3), may now be used to calculate the masses of primary fission products from which we may compare the *total* energy release in different modes of splitting. For example, the total mass of ${}_{40}Zr^{100}+{}_{52}Te^{136}$ is calculated to be 235.91051 amu and that of ${}_{46}Pd^{118}+{}_{46}Pd^{118}$ to be 235.91288 amu. The former is smaller than the latter by about 2 Mev. Thus the total energy release in the asymmetric mode ${}_{40}Zr^{100}+{}_{52}Te^{136}$ is about 2 Mev larger than that in the symmetric mode ${}_{46}Pd^{118}+{}_{46}Pd^{118}$. None of these nuclides are magic-number ones. It will be interesting to note that if the uncorrected mass formula, Eq. (1), is used for calculation, the total energy release in ${}_{46}Pd^{118}+{}_{46}Pd^{118}$ splitting would be calculated to be higher than that of ${}_{40}Zr^{100}+{}_{52}Te^{136}$ by 4.2 Mev.

III. NUCLEAR LEVEL DENSITY

The energy level density of a nucleus is usually expressed by a formula derived from the statistical model of nucleus,

$$W_0(E) = c\exp[2(aE)^{\frac{1}{2}}]. \tag{5}$$

The parameters a and c, as functions of the mass number A, have been determined empirically[25,26] by using experimental data of slow-neutron resonance level spacings. However, the results were considered as a rough approximation and good only for odd nuclides. As for the even nuclides, there are indications that they have smaller densities.[25] Recent studies show that the magic-number nuclides have abnormal level spacings.[27] In this section we shall use experimental data of fast-neutron capture cross sections[28] to determine the parameters a and c as functions of A.

[15] Coryell, Brightsen, and Pappas, Phys. Rev. **85**, 732 (1952).
[16] A. H. Wapstra, Physica **18**, 83 (1952).
[17] Collins, Nier, and Johnson, Phys. Rev. **86**, 408 (1952).
[18] A. E. S. Green and N. A. Engler, Phys. Rev. **91**, 40 (1953); A. E. S. Green and D. F. Edwards, Phys. Rev. **91**, 46 (1953).
[19] K. Way, Atomic Energy Commission Report CP-2497, 1944 (unpublished).
[20] I. Joliot-Curie, J. phys. radium (8), **6**, 209 (1945).
[21] E. Feenberg, Revs. Modern Phys. **19**, 329 (1947).
[22] T. P. Kohman, Phys. Rev. **73**, 16 (1948).
[23] W. H. Sullivan, *Trilinear Chart of Nuclear Species* (John Wiley and Sons, Inc., New York, 1949).
[24] J. R. Stehn, Phys. Rev. **93**, 932 (1954).
[25] Feld, Feshbach, Goldberger, Goldstein, and Weisskopf, U. S. Atomic Energy Commission NYO-636, 1951 (unpublished), pp. 176, 185.
[26] J. M. Blatt and V. F. Weisskopf, Office of Naval Research Report ONR-42, 1950 (unpublished), p. 60.
[27] H. W. Newson and R. H. Rohrer, Phys. Rev. **87**, 177 (1952). This paper gives the slow-neutron data. For fast-neutron data, see reference 28 below. For level spacing near ground states, see F. Asaro and I. Perlman, Phys. Rev. **87**, 393 (1952); P. Staehelin and P. Preiswerk, Helv. Phys. Acta **24**, 623 (1952); P. J. Grant, Proc. Phys. Soc. (London) **A65**, 150 (1952); B. B. Kinsey, quoted in reference 31.
[28] Hughes, Spatz, and Goldstein, Phys. Rev. **75**, 1781 (1949). This paper gives references to earlier work. D. J. Hughes and D. Sherman, Phys. Rev. **78**, 632 (1950); Hughes, Garth, and Eggler, Phys. Rev. **83**, 234 (1951) and "Fast-Neutron Cross Sections and Nuclear Level Density" (unpublished); Garth, Hughes, and Palevsky, Brookhaven National Laboratory Report BNL-103, 1950 (unpublished), p. 24; Garth, Hughes, and Levin, Phys. Rev. **87**, 222 (1952). Hughes, Garth, and Levin, Phys. Rev. **91**, 1423 (1953).

The fast-neutron capture cross section is related to the level density by the following formula derived from the statistical theory of nuclear reactions[29]:

$$\sigma_c = (2\pi^2/k^2)\Gamma_\gamma W_0, \tag{6}$$

where k is the neutron wave number, Γ_γ is the radiation width, and W_0 is the density of levels due to neutrons of zero angular momentum. Since the capture cross sections used below are due mainly to the contributions of neutrons of zero angular momentum,[28] Eq. (6) may be used to determine W_0. For σ_c, the capture cross-section data of 1-Mev neutrons by Hughes *et al.*[28] are used. The values of Γ_γ are taken from the straight-line extrapolation of the values of Heidmann and Bethe.[30] The value of k corresponds to the wave number of 1-Mev neutrons. From these values we calculated the values of W_0 for 42 compound nuclei formed by capturing a 1-Mev neutron.

In order to determine the quantities a and c occurring in Eq. (5), the energies E of the compound nuclei must be determined. The ground-state level position varies discontinuously from one isotope to the other due to the δ_A and μ terms in Eq. (3); Hurwitz and Bethe[31] have pointed out that these fluctuations may not eixst in high excited states. In order to correlate the neutron capture cross sections to the neutron binding energies, they found it necessary to propose that the energy E of the compound nucleus in Eq. (5) is not to be measured from the ground state of the excited nucleus but from a "characteristic level" of the same which is free from the even-odd and magic-number effects and so varies smoothly from one isotope to the other. The fluctuation of the ground-state level is then attributed to some factors which have a strong influence on the ground and low-lying states but have little influence on the high excited states.[31] According to this hypothesis the E values so measured are not determined by the binding energy of the last neutron of the *compound* nucleus but instead by the total energy content of the initial system of the *target* nucleus plus a free neutron. Hurwitz and Bethe pointed out that the neutron capture cross section, which is proportional to the level density, actually varies according to this pattern. The experiments of Harris *et al.*[32] show that the level densities of odd-even and even-odd *target* nuclei, which correspond to odd-odd and even-even compound nuclei, are nearly equal. This is in agreement with the prediction of the Hurwitz-Bethe hypothesis. Evidence from the magic-number nuclei also provides a test in favor of this hypothesis. On the basis of these considerations, the Hurwitz-Bethe hypothesis will be assumed for the present work.

The next problem is to determine the position of the characteristic level, which should be smooth and free from the even-odd and magic-number effects. Hurwitz and Bethe[31] suggested that the characteristic level probably may be represented by a level calculated from the liquid-drop model mass formula excluding the even-odd energy δ_A term. In using our modified mass formula, Eq. (3), the discontinuous μ term should be excluded also. Without the δ_A and μ terms Eq. (3) is a continuous, smoothly varying function of A and Z, free from fluctuations due to even-odd and magic-number effects and so may be used as the characteristic energy level of any nucleus. However, the absolute position of the characteristic levels is not determined in the previous considerations. This leaves free a constant (or nearly constant) term in the expression for the characteristic level which has to be fixed by other considerations. It has been assumed in the following calculations that the characteristic level of all nuclei coincides with the ground state of the odd-odd nuclei, i.e.,

$$M^c(A,Z) = M_A + \Delta M_A + B_A(Z - Z_A - \Delta Z_A)^2 + 0.036/A^{\frac{2}{3}} \text{ amu}, \tag{7}$$

where ΔM_A and ΔZ_A are given by Fig. 3 and Fig. 2.

The excitation energy E of a compound nucleus measured from its characteristic level may now be calculated as follows: First calculate the energy content of the initial system of a target nucleus [by Eq. (3)] plus a free neutron. Then subtract from it the mass of the compound nucleus at its characteristic level given by Eq. (7). The values of excitation energies E so obtained and level densities W_0 previously determined may be put into Eq. (5) to determine the parameters a and c. However, for each nucleus we have only one equation to determine two parameters a and c. In order to determine a and c separately, we make the assumption that two neighboring nuclides A_1 and A_2 have essentially the same parameters a, c, and Γ_γ. The logarithm of the ratio of their neutron capture cross sections will then, according to Eqs. (5) and (6), be given by

$$\ln[\sigma(A_1)/\sigma(A_2)] = 2\sqrt{a}(\sqrt{E_1} - \sqrt{E_2}).$$

Since E_1 and E_2 are known, a can be determined. Unfortunately, this is applicable only when the excitation energies of the two neighboring nuclides differ appreciably. Otherwise, a large error will be introduced. From a few pairs of nuclides satisfying this condition the parameter a is determined for the corresponding masses. A plot of a *versus* A is made and a straight line may be drawn passing through the points. This line may be represented by the formula

$$a = 0.050A, \tag{8}$$

which may be considered as a first approximation. Using the values of a given by Eq. (8) we can determine the values of the other parameter c for the 42 nuclides

[29] Feshbach, Peaslee, and Weisskopf, Phys. Rev. **71**, 145 (1947).
[30] J. Heidmann and H. A. Bethe, Phys. Rev. **84**, 274 (1951).
[31] H. Hurwitz and H. A. Bethe, Phys. Rev. **81**, 898 (1951).
[32] Harris, Muehlhause, and Thomas, Phys. Rev. **79**, 11 (1950), and Bollinger, Harris, Hibdon, and Muehlhause, Phys. Rev. **92**, 1527 (1953).

previously mentioned. A straight line is drawn on a logarithmic plot of *c versus A*. The mass dependence of c may be expressed as follows:

$$c=0.38e^{-0.005A}. \tag{9}$$

This is also a first approximation. Since the parameter c, as will be seen later, is less important than the other parameter a in this work, we shall assume the c values of Eq. (9) to be correct. Using these values, we can calculate the values of the parameter a for the 42 nuclides. The results are plotted against the mass number A in Fig. 4. The straight line represents Eq. (8). It is seen that Eq. (8) represents the variation of a with respect to mass number fairly well. Therefore, we shall use Eqs. (8) and (9) for the level density parameters a and c. They hold for all types of nuclides, even, odd or magic. The discontinuous changes due to even-odd and magic-number effects are attributed to the change of excitation energy instead of change of level density parameters. The linearity of the parameter a with respect to mass number also agrees with the result of the statistical model of nucleus.

Equation (5) with its parameters given by Eqs. (8) and (9) represents only the density of levels resulting from the capture of neutrons of zero angular momentum. For convenience, it is identified with the density of levels of zero angular momentum. To obtain the density of levels with different angular momenta we use the formula given by Bethe,[33]

$$W_j(E)=(2j+1)\exp[-(j+\tfrac{1}{2})^2/2gT]W_0(E), \tag{10}$$

where g and T are given by

$$\begin{aligned} g&=\tfrac{2}{5}(MR^2/\hbar^2)\sim A^{5/3},\\ T&=(E/a)^{\frac{1}{2}}, \end{aligned} \tag{11}$$

where M and R are the mass and radius of the nucleus of mass number A, and T is the nuclear temperature. For a nucleus of mass number 120 excited to 10 Mev, this formula gives a most probable value of j to be about 10. This formula does not include the multiplicity due to the orientation of the angular momentum vector; it will be seen later that the j dependence is rather unimportant for our purpose.

IV. INTERNAL ENERGY AVAILABLE AT THE INSTANT OF SEPARATION

Knowing the masses of primary fission fragments and the mass of the initial system, we can calculate the energy F released in the fission process by the following formula:

$$F=M^*(A,Z)-M(A_1,Z_1)-M(A_2,Z_2), \tag{12}$$

where $M^*(A,Z)$ is the mass of the excited compound nucleus undergoing fission, and $M(A_1,Z_1)$ and $M(A_2,Z_2)$ are the masses of primary fission fragments in their ground states. The sum of A_1 and A_2 is A and the sum of Z_1 and Z_2 is Z. F is the total energy release excluding the subsequent energy release through beta transformations of the primary fission products. The mass of U^{235} is taken to be 235.11794±100 amu, which is derived from the experimental mass of Pb^{208} [34] and the mass difference between Pb^{208} and U^{235}.[35] The value of M^* for fission of U^{235} with thermal neutrons is $M(235,92)+N$, which is 236.12692 amu. The masses of fission products may be calculated from Eq. (3). Thus the energy F released in asymmetric fission ${}_{40}Zr^{100}+{}_{52}Te^{136}$ is 0.21641 amu or 201.48 Mev. That of symmetric fission ${}_{46}Pd^{118}+{}_{46}Pd^{118}$ is 0.21404 amu or 199.27 Mev, about 2 Mev less than that of asymmetric fission.

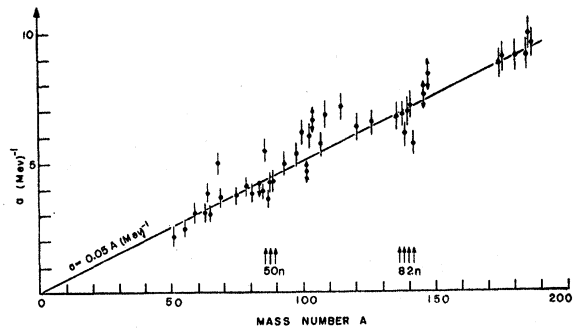

FIG. 4. Mass dependence of the level density parameter a.

We are interested in the excitation energy of the fission fragments at the critical moment, approximated by two deformed nuclei in contact. Between the two fragments there exists a mutual Coulomb energy, C. In addition, each of the fragments possesses an amount of deformation energy. (According to the L.D.M., a deformed nucleus has a larger surface energy and a smaller Coulomb energy than the spherical nucleus. The net change is a positive quantity, which is the deformation energy.) We denote the deformation energies by D_1 (light fragment) and D_2 (heavy fragment). The sum of D_1 and D_2 is denoted by D. The sum of C and D is the total potential energy, P, of this nuclear configuration,

$$P=C+D. \tag{13}$$

The difference $F-P$, denoted by G, is then the energy available for internal excitation and center-of-gravity motion of the fragments at the critical moment. The total internal excitation energy of both fragments is denoted by E and the total translational motion energy is denoted by k. The above relations may be expressed as follows:

$$\begin{aligned} F&=P+G\\ &=C+D+E+k. \end{aligned} \tag{14}$$

In Sec. V it will be shown that a given G may be divided in many ways into E and k but in general $E\gg k$.

[33] H. A. Bethe, Revs. Modern Phys. 9, 79 (1937).

[34] Stanford, Duckworth, Hogg, and Geiger, Phys. Rev. 85, 1039 (1952).

[35] M. O. Stern, quoted from R. B. Leachman, Phys. Rev. 87, 444 (1952).

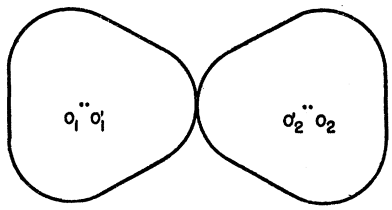

FIG. 5. Most probable deformation shape of symmetric fission of compound nucleus U^{236}, just before the fragments separate, calculated on the basis of $P_3(\cos\theta)$ deformation only.

The maximum value of E is G for the special case of $k=0$. Thus, G may be called the *maximum excitation energy*. The potential energies may be calculated by using the liquid drop model. From the potential energies the maximum excitation energy G may be calculated. From G, as will be shown in Sec. V the relative fission probability may be calculated. In the following we present a calculation of the potential energy.

We assume the nuclear matter to be an incompressible liquid drop with uniform mass and charge density. In order to calculate the mutual Coulomb energy and deformation energies we have to know the deformation shape of each fragment and their relative positions. While we assume the fission fragments to be deformed, there is no reason to assume a unique deformation shape for all fragments. Many deformation shapes may be possible and so many sets of values of C, D_1, and D_2. According to the statistical assumption, each deformation configuration will occur with a probability proportional to its density of quantum states. Thus, we have probability distributions of C, D_1, and D_2. The most general deformation shape of a liquid drop may be represented by a series expansion of the radius vector in Legendre Polynomials,

$$r(\theta)=r_0[1+\alpha_2P_2(\cos\theta)+\alpha_3P_3(\cos\theta)+\cdots]. \quad (15)$$

For simplicity we assume that the deformation of each fragment is due to the P_3 term only and that, at the moment just before separation, the two deformed nuclei are in contact at their tips and oriented such that their axes coincide. This is graphically represented in Fig. 5. The P_3 term is chosen because the corresponding deformed shape roughly approximates the egg-shaped fragment resulting from scission of a dumbbell-shaped parent nucleus. The shape of one fragment is thus specified by a single coefficient α_3 and its undeformed radius r_0. We shall use a second index i to specify the light fragment ($i=1$) or heavy fragment ($i=2$).

An approximate formula for the mutual Coulomb energy between the two fragments in the foregoing specified configuration is

$$C(\alpha_{31},\alpha_{32})=\frac{Z_1Z_2e^2}{r_{01}(1+0.9314\alpha_{31})+r_{02}(1+0.9314\alpha_{32})}. \quad (16)$$

The derivation of this formula is given in the appendix. For numerical calculation r_0 is taken as $1.5\times10^{-13}A^{\frac{1}{3}}$.

The deformation energies D_1 and D_2 may be obtained from an expression by Present and Knipp.[36] Neglecting cubic terms in α_3, the deformation energy of the ith fragment due to the P_3 deformation is

$$D_i(\alpha_{3i})=0.7143\alpha_{3i}^2E_{si}^0-0.2041\alpha_{3i}^2E_{ci}^0, \quad i=1,2, \quad (17)$$

where E_{si}^0 and E_{ci}^0 are the undeformed surface and electrostatic energies for the ith fragment. The values of E_{si}^0 and E_{ci}^0 are calculated from $E_s^0=0.014A^{\frac{2}{3}}$ amu and $E_c^0=0.000627Z^2/A^{\frac{1}{3}}$ amu according to Fermi's liquid-drop model mass formula.[6]

Thus we have expressed P in terms of α_{31} and α_{32}. There will be one such potential function $P(\alpha_{31},\alpha_{32})$ for each mass and charge division. It will be shown in Sec. V that the deformation shape which gives minimum potential energy, and therefore maximum internal excitation energy, is the most probable one to occur. Consequently for fission leading to given mass and charge division the most probable values of Coulomb and deformation energy are obtained by minimizing $P(\alpha_{31},\alpha_{32})$. The minimum may be found numerically. Such a calculation is carried out for the fission of U^{235} with slow neutrons. The calculation is made at a number of mass splittings each having its charge split at the most probable charges (see Sec. V for most probable charges). The most probable deformation coefficients α_{31} and α_{32} thus obtained are nearly equal and slowly varying with respect to mass number. Thus the most probable deformation shapes of the two fragments, disregarding the size proportion, are roughly the same and change only little from one mass splitting to the other. The most probable α_{31} and α_{32} of symmetric fission are both 0.1975. The corre-

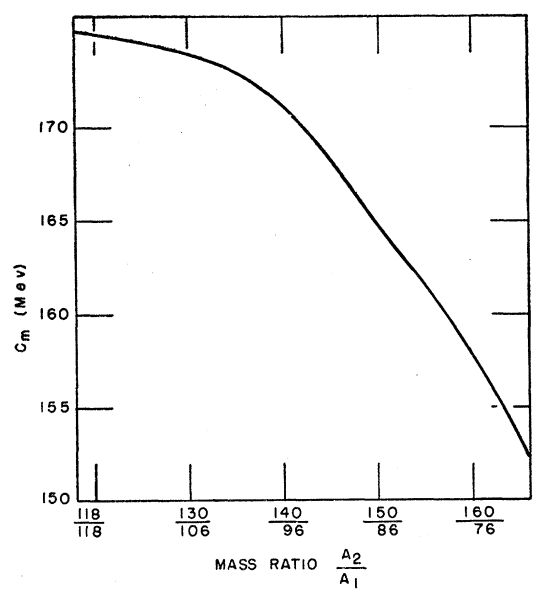

FIG. 6. Most probable Coulomb energy C_m of a pair of fission fragments from the compound nucleus U^{236} as a function of mass ratio of splitting.

[36] R. D. Present and J. K. Knipp, Phys. Rev. 57, 751 (1940).

sponding deformation shape is given in Fig. 5. The most probable Coulomb energy C for different mass splittings is calculated and plotted as a function of mass ratio of splitting in Fig. 6. It is a monotonically decreasing function and its value for symmetric fission is 175.2 Mev. The most probable deformation energies D_1 and D_2 are also calculated and plotted as functions of mass number in Fig. 7. They are nearly constant with respect to the mass numbers A_1 and A_2. Their value for symmetric fission is 6.73 Mev.

The mutual Coulomb energy has a maximum for symmetric fission. Therefore, the term C favors asymmetric fission. On the other hand, the total deformation energy is nearly constant. Therefore, the term D does not essentially affect the asymmetry of mass splitting. Although these are results of an approximate calculation of the potential energies, other approximate calculations also lead to the same conclusions. They will be discussed in the appendix.

We have calculated the potential energies at the critical moment. After the two fragments separate from each other the mutual Coulomb energy becomes the kinetic energy of the fragments and the deformation energies become internal excitation energies of the fragments. Therefore, when the two fragments are separated by an infinite distance, the total kinetic energy of the fragments will be $K=C+k$ and the total internal excitation energies of the fragments will be $H=D+E$. The distributions of C and D will result in distributions of K and H. The latter may be compared with experimental information on K and H (Sec. VII).

V. RELATIVE PROBABILITIES OF FISSION MODES

The relative probability of a fission mode is assumed to be proportional to the density of quantum states. It will be seen that the density of quantum states depends on the mass numbers, charge numbers, and deformation shapes of the fission fragments. By integration over the deformation shapes we obtain the relative probability of the fission mode specified by given mass

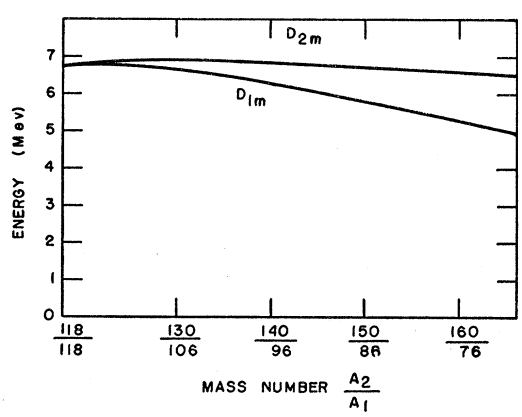

FIG. 7. Most probable deformation energies D_{1m} of light fragment and D_{2m} of heavy fragment from compound nucleus U^{236} as functions of mass numbers A_1 and A_2, respectively.

and charge numbers. By integrating this over the charge numbers we have the relative probability of a given mass ratio. This is the mass distribution which must be compared with the experimental results.

The nuclear configuration at the moment just before separation consists of two deformed nuclei in contact. The excitation energy E gives rise to a number of excitation states and the translational energy k gives rise to a number of momentum states. The density of quantum states is a product of these two. As the system is isolated, its energy, linear momentum and angular momentum must be conserved; we proceed to calculate the density of quantum states subject to these conditions.

a. Density of Excitation States

Consider a system consisting of two thermally interacting components, each of which has a number of quantum states represented by a level density expression $\rho_1(\epsilon_1)$ and $\rho_2(\epsilon_2)$ respectively. Let the total energy of the system be ϵ and the density of quantum states of the whole system be N. We have

$$N=\int_0^{\epsilon}\rho_1(\epsilon_1)\rho_2(\epsilon-\epsilon_1)d\epsilon_1. \tag{18}$$

Equation (18) may be interpreted as meaning that the density of quantum states of a compound system is the sum of all partial densities, $\rho_1(\epsilon_1)\rho_2(\epsilon-\epsilon_1)d\epsilon_1$, each corresponding to a partition of energy ϵ into ϵ_1 and ϵ_2 between the two components. The statistical assumption asserts that the partial densities will represent the partial probabilities of occurrence of the corresponding partition of energy $\epsilon_1:\epsilon_2$.

The formula for the density of levels of an excited nucleus is discussed in Sec. III. It depends on the volume of the nucleus, but not on its shape. Since it was assumed that the deformed fission fragments have normal nuclear density, Eq. (5) is applicable. Let the total available excitation energy measured from the characteristic levels be E. Consider, at first, only excitation states of zero angular momentum. The density of excitation states of the two-nucleus system is, according to Eq. (18),

$$\Omega_0(E)=\int_0^E c_1\exp[2(a_1E_1)^{\frac{1}{2}}]c_2 \times\exp\{2[a_2(E-E_1)]^{\frac{1}{2}}\}dE_1. \tag{19}$$

Conservation of angular momentum is satisfied if the fissioning nucleus has zero angular momentum.

Equation (19) cannot be integrated exactly. As the integrand is a rapidly varying function, the integral is determined essentially by the integration in the neighborhood of the maximum of the integrand. The integrand in this region behaves like a Gaussian; the

approximating Gaussian is integrated, and the result is

$$\Omega_0(E)=2\pi^{\frac{1}{2}}c_1c_2\frac{(a_1a_2)^{\frac{1}{2}}}{(a_1+a_2)^{5/4}}E^{\frac{3}{4}}\exp\{2[(a_1+a_2)E]^{\frac{1}{2}}\}. \quad (20)$$

It will be noted that the maximum of the integrand corresponds to a partition of E into E_1 and E_2 such that the two fragments have equal nuclear temperature. This is expected from the condition of equilibrium.

Next we consider the excitation states of higher angular momentum, the density of which is given by Eq. (10). We consider the case in which the initial angular momentum of the compound nucleus undergoing fission is zero, and there exists no orbital angular momentum between the two fission fragments. Conservation of angular momentum requires that the resultant of the angular momenta of the two fragments must be zero. Thus we have the total density of excitation states:

$$\begin{aligned}\Omega(E)&=\sum_j(2j+1)^2\exp\left[-(j+\tfrac{1}{2})^2\left(\frac{1}{2g_1T_1}+\frac{1}{2g_2T_2}\right)\right]\Omega_0(E)\\&\cong\pi^{\frac{1}{2}}(gT)^{\frac{3}{2}}\Omega_0(E)\\&\sim\left(\frac{A_1^{5/3}A_2^{5/3}}{A_1^{5/3}+A_2^{5/3}}\right)^{\frac{3}{2}}\left(\frac{E_1+E_2}{a_1+a_2}\right)^{\frac{3}{4}}\Omega_0(E)\\&\sim c_1c_2\left(\frac{A_1^{5/3}A_2^{5/3}}{A_1^{5/3}+A_2^{5/3}}\right)^{\frac{3}{2}}\frac{(a_1a_2)^{\frac{1}{2}}}{(a_1+a_2)^2}E^{\frac{3}{2}}\\&\qquad\times\exp\{2[(a_1+a_2)E]^{\frac{1}{2}}\},\end{aligned} \quad (21)$$

where $(1/g)\equiv(1/g_1)+(1/g_2)$. It is assumed that $T_1=T_2=T$ and the summation is approximated by an integration.

For the more general case where the angular momentum of the compound nucleus is not zero and orbital angular momentum exists between the two fragments, it can be shown[37] that the results differ from Eq. (21) by a slowly varying factor only. The dominant exponential factor remains unchanged.

b. Density of Momentum States

At the moment just before separation, the momenta of the two fragments due to the motion of their centers of gravity must be equal and opposite. Let their absolute values be p. The energy of translational motion k is

$$k=(1/2m_1)p^2+(1/2m_2)p^2, \quad (22)$$

where m_1 and m_2 are the masses of the two fragments. Since the momenta of the two fragments are equal and opposite, the number of momentum states of the two-fragment system is equal to that of one fragment. Therefore the density of momentum states of the two-fragment system is

$$\omega(k)=\frac{4\pi V}{h^3}(2m^3k)^{\frac{1}{2}}, \quad (23)$$

where m is given by

$$m=\frac{m_1m_2}{m_1+m_2}\sim\frac{A_1A_2}{A_1+A_2}. \quad (24)$$

c. Total Density of Quantum States

The total density of quantum states of the two-nucleus system is a product of densities of excitation states and momentum states. When statistical equilibrium is established we may consider the excitation and the translational motion as two thermally interacting components between which the energy may be exchanged. The total energy available to the whole system is G. Equation (18) gives the total density of quantum states of the system

$$Q(G)=\int_0^G\Omega(G-k)\omega(k)dk=\int_0^G\Omega(E)\omega(G-E)dE. \quad (25)$$

In Eq. (21), $\Omega(E)$ is expressed in terms of E, measured from the characteristic level. G in Eq. (25), being the maximum possible value of E, is also to be measured from the characteristic level. Thus we have

$$\begin{aligned}Q(G')\sim\int_0^{G'}c_1c_2\left(\frac{A_1^{5/3}A_2^{5/3}}{A_1^{5/3}+A_2^{5/3}}\right)^{\frac{3}{2}}\frac{(a_1a_2)^{\frac{1}{2}}}{(a_1+a_2)^2}E^{\frac{3}{2}}\\\times\exp\{2[(a_1+a_2)E]^{\frac{1}{2}}\}[2m^3(G'-E)]^{\frac{1}{2}}dE,\end{aligned} \quad (26)$$

where G' is the value of G measured from the characteristic level,

$$\begin{aligned}G'=M^*(A,Z)-M^c(A_1,Z_1)\\-M^c(A_2Z_2)-P(\alpha_{31},\alpha_{32}).\end{aligned} \quad (27)$$

While the integral of Eq. (25) gives the total density of quantum states, the integrand of Eq. (25) gives the partial density of quantum states corresponding to a given partition of G into E and k. According to the statistical assumption, the integrand gives the distribution function of E or of k. The most probable partition of G can be determined by maximizing the integrand. The maximum condition is an equation of the fourth order, an approximate solution of which is

$$k_0=\frac{1}{2}\left(\frac{G'}{a_1+a_2}\right)^{\frac{1}{2}}\left(1-\frac{7}{4}\frac{1}{[(a_1+a_2)G']^{\frac{1}{2}}}+\cdots\right). \quad (28)$$

k_0 is thus the most probable translational energy of the centers of gravity of the two fragments at the moment just before separation. Equation (28) shows that only a small fraction of G, of the order of 0.5 Mev, is given to k. This is due to the fact that the partition of energy is determined by the number of degrees of freedom. The

[37] P. Fong, Ph.D. dissertation, University of Chicago, 1953 (unpublished).

translational motion has only three degrees of freedom while the excitation motion has many more. As k_0 is small compared to Coulomb energy C, we shall neglect the distribution in translational energy and assume that the value of k is given by a single value k_0 expressed in Eq. (28).

Returning to Eq. (26), we find the integration is largely determined by the integrand in the neighborhood of its maximum and so can be simplified by replacing the slowly varying factors of the integrand by their values at the maximum. The remaining exponential factor is then integrated. The result is, neglecting small quantities,

$$Q(G')\sim c_1c_2\left(\frac{A_1^{5/3}A_2^{5/3}}{A_1^{5/3}+A_2^{5/3}}\right)^{\frac{3}{2}}\left(\frac{A_1A_2}{A_1+A_2}\right)^{\frac{3}{2}}\times\frac{(a_1a_2)^{\frac{1}{2}}}{(a_1+a_2)^{11/4}}(G')^{9/4}\left(1-\frac{19}{8}\frac{1}{[(a_1+a_2)G']^{\frac{1}{2}}}\right)\times\exp\{2[(a_1+a_2)G']^{\frac{1}{2}}\}. \quad (29)$$

Equation (29) gives the total density of quantum states of a two-nucleus system in terms of mass numbers, level density parameters and the maximum excitation energy G'. This equation will be used to calculate the relative probabilities of fission modes.

The maximum excitation energy G' depends, according to Eq. (27), on the mass and charge numbers and the deformation shapes of the two fission fragments. Therefore the relative fission probability depends on these quantities and there will be mass, charge, and deformation shape distributions.

d. Coulomb Energy Distribution

Consider a given mass and charge division $(A_1,Z_1):(A_2,Z_2)$. Equation (29), which depends on the Coulomb energy and deformation energy through G', gives a probability distribution of the deformation shapes and so probability distributions of C and D. We shall discuss the distribution of C, which, after adding the negligibly small k_0 (less than 1% of C), will give the distribution of *final* kinetic energy of fission fragments and may be compared with the experimental results.

When the mass and charge ratios of splitting are fixed Eq. (29) may be simplified to give the probability distribution of deformation shapes,

$$N(\alpha_{31},\alpha_{32};A_1,A_2,Z_1,Z_2)\sim(G')^{9/4}\left(1-\frac{19}{8}\frac{1}{[(a_1+a_2)G']^{\frac{1}{2}}}\right)\times\exp\{2[(a_1+a_2)G']^{\frac{1}{2}}\}. \quad (30)$$

There will be one such equation for each mass and charge division $(A_1,Z_1):(A_2,Z_2)$.

For any deformation shape $(\alpha_{31},\alpha_{32})$, Eq. (16) determines the Coulomb energy and Eq. (30) gives its corresponding probability of occurrence. However the correspondence between deformation shape and the Coulomb energy is not one-to-one. There exist many combinations of α_{31} and α_{32} which will give the same Coulomb energy $C(\alpha_{31},\alpha_{32})$. We shall consider only the most probable combination of α_{31} and α_{32} for a given Coulomb energy value (the inclusion of other combinations will not essentially change the final results). This combination may be obtained by maximizing G' with respect to α_{31} and α_{32} subject to the condition that $C(\alpha_{31},\alpha_{32})$ is constant. The relation between α_{31} and α_{32} for this combination is obtained to be

$$\frac{\alpha_{31}}{\alpha_{32}}=\frac{r_{01}}{r_{02}}\frac{(1.4286E_{s2}^0-0.4082E_{c2}^0)}{(1.4286E_{s1}^0-0.4082E_{c1}^0)}. \quad (31)$$

This relation reduces the number of independent deformation coefficients to one. Consequently, Coulomb energy and deformation shape may be correlated in a one-to-one manner. The Coulomb energy distribution may be derived as follows: We express the value of G' of Eq. (27) in the neighborhood of its maximum with respect to α_{31} as a parabolic function of $\delta\alpha_{31}$, the deviation of α_{31} from the maximum. Substituting G' into Eq. (30) we get a distribution function in terms of $\delta\alpha_{31}$, which is roughly a Gaussian function. The latter may be translated into a distribution function in terms of δC, the deviation of C from the most probable C, which again is roughly a Gaussian,

$$N(C;A_1,A_2,Z_1,Z_2)\sim\exp[-(\delta C/\Delta)^2], \quad (32)$$

where

$$\Delta\cong\frac{(dC/d\alpha_{31})_m}{\left\{\frac{1}{2}\left[\frac{d^2(C+D_1+D_2)}{d\alpha_{31}^2}\right]_m\right\}^{\frac{1}{2}}}\left\{\frac{G'}{\frac{9}{4}+[(a_1+a_2)G']^{\frac{1}{2}}}\right\}^{\frac{1}{2}}\text{ Mev}, \quad (33)$$

where the subscript m indicates that the values are to be taken at the most probable configuration. Equation (32) will be the Coulomb energy distribution function. The first factor in Δ depends on the mass and charge ratios of division and is nearly proportional to $(Z_1Z_2)^{\frac{1}{2}}$. Thus we have

$$\Delta\simeq\text{const}\,(Z_1Z_2)^{\frac{1}{2}}\times\left(\frac{G'}{a_1+a_2}\right)^{\frac{1}{4}}\left(1-\frac{9}{8}\frac{1}{[(a_1+a_2)G']^{\frac{1}{2}}}\right)\text{ Mev}. \quad (34)$$

e. Charge Distribution

Integrating over the Coulomb energy distribution curve, we have the total number of quantum states of the fission mode specified by a given mass and charge division. The area under the Coulomb energy distribution curve is proportional to the product of the Gaussian width Δ and the maximum ordinate of the Gaussian

curve. We obtain

$$N(A_1,A_2,Z_1,Z_2)$$
$$\sim c_1c_2\frac{(a_1a_2)^{\frac{1}{2}}}{(a_1+a_2)^{12/4}}\left(\frac{A_1^{5/3}A_2^{5/3}}{A_1^{5/3}+A_2^{5/3}}\right)^{\frac{3}{2}}\left(\frac{A_1A_2}{A_1+A_2}\right)^{\frac{3}{2}}$$
$$\times(Z_1Z_2)^{\frac{1}{2}}(G_m')^{10/4}\left\{1-\frac{7}{2}\frac{1}{[(a_1+a_2)G_m']^{\frac{1}{2}}}\right\}$$
$$\times\exp\{2[(a_1+a_2)G_m']^{\frac{1}{2}}\},\quad(35)$$

where G_m' is the value of G' calculated for the most probable mode in the Coulomb energy distribution,

$$G_m'=M^*(A,Z)-M^c(A_1,Z_1)-M^c(A_2,Z_2)$$
$$-C_m(Z_1,Z_2)-D_{1m}-D_{2m},\quad(36)$$

where C_m, D_{1m}, and D_{2m} are the most probable values of C, D_1, and D_2 with respect to α_{31} and α_{32} for given A_1, A_2, Z_1, and Z_2.

The relative probabilities of various charge divisions for a given mass division $A_1:A_2$ may be simplified as

$$N(Z_1,Z_2;A_1,A_2)$$
$$\sim(Z_1Z_2)^{\frac{1}{2}}\left\{1-\frac{7}{2}\frac{1}{[(a_1+a_2)G_m']^{\frac{1}{2}}}\right\}(G_m')^{10/4}$$
$$\times\exp\{2[(a_1+a_2)G_m']^{\frac{1}{2}}\}.\quad(37)$$

There will be a pair of such equations (36) and (37) for each given mass division $A_1:A_2$.

Equation (37) implies that the most probable charge division $Z_{p1}:Z_{p2}$ (nonintegral) is the one having maximum G_m'.[38] Thus the most probable charges may be obtained by maximizing Eq. (36) with respect to Z_1 and Z_2 under the condition $Z_1+Z_2=Z$. The variation of the total deformation energy with respect to charge division $Z_1:Z_2$ for fixed mass division can be shown to be very small. Thus $D_{1m}+D_{2m}$ may be regarded as constant. $C_m(Z_1,Z_2)$ is given by

$$C_m(Z_1,Z_2)=Z_1Z_2e^2/\{r_{01}[1+0.9314\alpha_{31m}]$$
$$+r_{02}[1+0.9314\alpha_{32m}]\},\quad(38)$$

where α_{31m} and α_{32m} are the most probable values of α_{31} and α_{32}. As α_{31m} and α_{32m}, determined in Sec. IV, are nearly constant, we have roughly

$$C_m(Z_1,Z_2)\cong c_{12}Z_1Z_2,\quad(39)$$

where c_{12} is a constant with respect to charge division. The value of c_{12} varies from 0.0889 mMU to 0.0910 mMU when the mass ratio varies from 1.00 to 2.33. Using the mass formula Eq. (7) we have the most probable charges, by maximizing Eq. (36),

$$Z_{p1}=\frac{B_{A1}(Z_{A1}+\Delta Z_{A1})-B_{A2}(Z_{A2}+\Delta Z_{A2})+Z(B_{A2}-\frac{1}{2}c_{12})}{B_{A1}+B_{A2}-c_{12}},$$
$$Z_{p2}=Z-Z_{p1}.\quad(40)$$

[38] The factor $(Z_1Z_2)^{\frac{1}{2}}$ is slowly varying and may be regarded as constant as far as the determination of the maximum is concerned.

With the most probable charges known, the excitation energies of all other modes of charge division may be related to that of the most probable mode as follows:

$$G_m'(Z_1,Z_2)=G_m'(Z_{p1},Z_{p2})$$
$$-(B_{A1}+B_{A2}-c_{12})(\Delta Z)^2,\quad(41)$$

where ΔZ is given by

$$\Delta Z=|Z_1-Z_{p1}|=|Z_2-Z_{p2}|.\quad(42)$$

We call ΔZ the charge displacement, the magnitude of which indicates how far the charge division $Z_1:Z_2$ deviates from the most probable division $Z_{p1}:Z_{p2}$.

The charge distribution function, giving relative probability as a function of charge displacement, may be derived by substituting Eq. (41) into Eq. (37). For ΔZ small, Eq. (37), neglecting small terms, gives roughly a Gaussian curve in ΔZ,

$$N(Z_1,Z_2;A_1,A_2)\sim\exp[-(\Delta Z/\delta)^2],\quad(43)$$

where the width δ is

$$\delta=\frac{1}{[B_{A1}+B_{A2}-c_{12}]^{\frac{1}{2}}}\left(\frac{G_m'(Z_{p1},Z_{p2})}{a_1+a_2}\right)^{\frac{1}{4}}$$
$$\times\left\{1-\frac{5}{4}\frac{1}{[(a_1+a_2)G_m'(Z_{p1},Z_{p2})]^{\frac{1}{2}}}\right\}\text{charge units.}\quad(44)$$

f. Mass Distribution

Integrating the number of quantum states over all possible charge distributions, we finally obtain the total number of quantum states at the moment of fission for any mass ratio $A_1:A_2$. This quantity we wish to identify with the relative probability of this mode of fission. Using the same method of integration as in the Coulomb energy distribution, we have

$$N(A_1,A_2)\sim c_1c_2\frac{(a_1a_2)^{\frac{1}{2}}}{(a_1+a_2)^{13/4}}\left(\frac{A_1^{5/3}A_2^{5/3}}{A_1^{5/3}+A_2^{5/3}}\right)^{\frac{3}{2}}$$
$$\times\left(\frac{A_1A_2}{A_1+A_2}\right)^{\frac{3}{2}}\frac{(Z_{p1}Z_{p2})^{\frac{1}{2}}}{(B_{A1}+B_{A2}-c_{12})^{\frac{1}{2}}}$$
$$\times(G_{mm}')^{11/4}\left(1-\frac{19}{4}\frac{1}{[(a_1+a_2)G_{mm}']^{\frac{1}{2}}}\right)$$
$$\times\exp\{2[(a_1+a_2)G_{mm}']^{\frac{1}{2}}\},\quad(45)$$

where G_{mm}' is the value of G_m' calculated for the most probable charge distribution,

$$G_{mm}'=M^*(A,Z)-M^c(A_1,Z_{p1})-M^c(A_2,Z_{p2})$$
$$-C_m(Z_{p1},Z_{p2})-D_{1m}-D_{2m}.\quad(46)$$

$C_m(Z_{p1},Z_{p2})$ is given in Fig. 6. D_{1m} and D_{2m} are given in Fig. 7. Equation (45) gives the mass distribution of the *primary* fission products. The dominant factor in Eq. (45) is the exponential one which does not change

from Eq. (20) on. This term varies by a factor of 10^2. The $(G_{mm}')^{11/4}$ factor varies by a factor of 10 while all other factors together vary by a factor of 2. As the value of a_1+a_2 in the exponent is constant, the mass distribution is essentially determined by the maximum excitation energy G_{mm}'. That the fission probability is determined mainly by the excitation energy, a rather small portion of the energy released in fission, is due to the fact that most of the degrees of freedom of the system are associated with this part of the fission energy.

VI. ASYMMETRIC FISSION

The experimental mass distribution curve has two pronounced peaks indicating the asymmetric splitting in fission. We shall derive, using Eq. (45) and Eq. (46), the mass distribution curve of U^{235} undergoing fission with slow neutrons and compare it with the experimental results.

The curve for the maximum excitation energy G_{mm}' *versus* mass ratio $A_1:A_2$ is calculated according to Eq. (46) and is plotted in Fig. 8. The value of G_{mm}' at symmetric fission is 6.86 Mev and that at the peak (asymmetric fission) is 11.97 Mev. With the G_{mm}' values known, Eq. (45) gives the mass distribution of *primary* fission products. However, the emission of prompt neutrons changes the mass numbers slightly. The average number of prompt neutrons emitted by a given fragment (of the order of 1) may be calculated from the values of the final excitation energy H. Changing the mass numbers accordingly, we obtain the mass distribution of the *final* fission products. The result is plotted in Fig. 9 and is compared with the observed yields of *final* fission products. The experimental data are taken from the summary of radiochemical data by Coryell and Sugarman[2] and the summary of mass-spectroscopic data by Glendenin *et al.*[39] The double-humped shape is reproduced and the agreement is generally satisfactory.

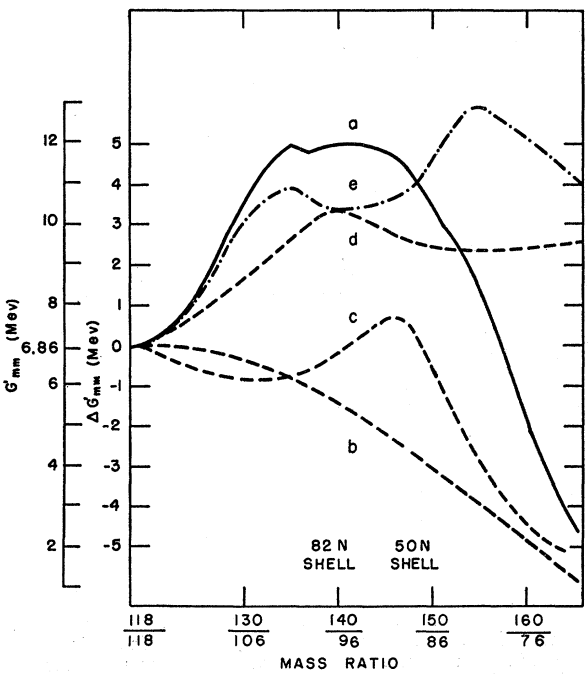

FIG. 8. Curve a: Maximum excitation energy G_{mm}' as a function of mass ratio of splitting of compound nucleus U^{236}. Curve b: Maximum excitation energy calculated according to the original liquid drop model mass formula without corrections ΔM_A and ΔZ_A. Curves c and d: The contribution to G_{mm}', due to the correction term ΔM_A, from the light and heavy fragments, respectively. Curve e. The contribution to G_{mm}' due to the correction term ΔZ_A. Curve a is the sum of curves b, c, d, and e.

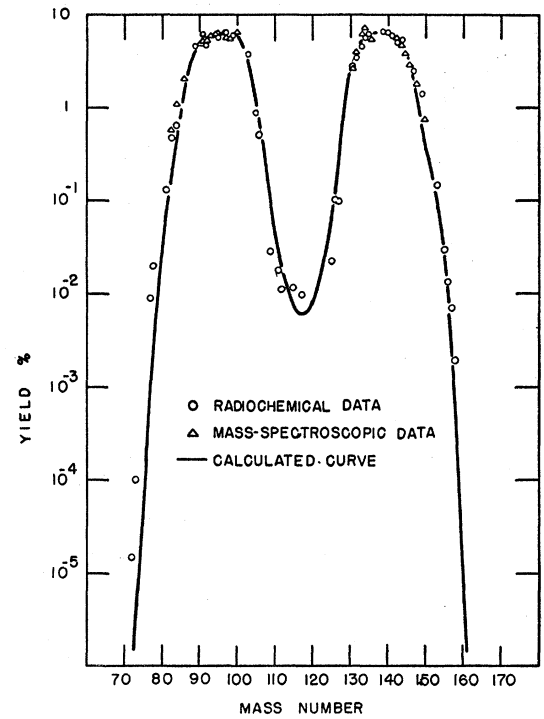

FIG. 9. Calculated mass distribution curve of fission products of U^{235} induced by thermal neutrons, compared with experimental data.

As the relative probability, given by Eq. (45), is a monotonically increasing function of the maximum excitation energy G_{mm}', the pronounced peaks of the mass distribution curve are essentially due to the peak of the G_{mm}' curve in the asymmetric fission region. It is important to note that, if the mass corrections ΔM_A and ΔZ_A were not included in the liquid-drop model mass formula, the peak of the G_{mm}' curve would be found at symmetric fission and symmetric fission would be the most probable. Thus the "cause" of asymmetric fission must be related to ΔM_A and ΔZ_A. We may divide the excitation energy into parts, separating the contributions due to ΔM_A and ΔZ_A from the energy calculated by using the original liquid-drop model mass formula. The G_{mm}' curve in Fig. 8 is thus resolved into

[39] Glendenin, Steinberg, Inghram, and Hess, Phys. Rev. 84, 860 (1951).

four components: curve b represents the value of G_{mm}' calculated according to the original liquid-drop model mass formula without corrections, curves c and d represent the contribution to G_{mm}' of the correction ΔM_A applied to light fragments and heavy fragments respectively, and curve e represents that of the correction ΔZ_A. When we add up all four curves we have the curve a which is calculated according to the corrected mass formula. The peak of curve a in the asymmetric fission region is due to the superposition of peaks of curves c, d, and e in the asymmetric region. The peaks in curves c and d are due to the extra stability of nuclear masses in the broad neighborhood of 50-neutron and 82-neutron shell edges. The peaks in curve d are due to the change of the beta-stability line as a result of the 50-neutron, 50-proton, and 82-neutron shells. In this sense nuclear shell structure is the "cause" of asymmetric fission.[40–42]

Many other factors contribute to the determination of mass distribution through Eq. (45) and Eq. (46). They do not essentially affect the asymmetry of splitting. Equation (46) contains the following:

(1) The mass of the fissioning nucleus. $M^*(A,Z)$ is a constant. A different value merely pushes the maximum excitation energy curve up or down while the peak in the asymmetric region remains unshifted.

(2) Masses of fission fragments. As mentioned above, these are mainly responsible for asymmetric fission. In our calculation, the excitation energy obtained is based on the masses of fragments at characteristic levels. If based on mass values at the ground-state levels, the excitation energies of fission fragments with 82 and 50 neutrons (in the peak yield region) will be *even higher* by 2 Mev, and those of fragments with 50 protons (in the symmetric fission region) will be also higher by 1 Mev. The net result is a small perturbation of the shape of the maximum excitation energy curve. The pronounced peak in the asymmetric region remains the same. Thus the use of characteristic levels is not critically related to the prediction of asymmetric fission.

(3) Coulomb energy. The Coulomb energy expression used here is calculated with some simplifying assumptions of nuclear deformation. Its main feature is that it is a monotonically decreasing function of the mass ratio because of the $Z_1 \cdot Z_2$ dependence. Therefore the Coulomb energy term in Eq. (46) favors asymmetric fission. However, unlike the ΔM_A and ΔZ_A terms, which favor the asymmetric fission rather abruptly in a particular mass ratio region, this term favors asymmetric fission rather uniformly over the whole mass ratio scale. Thus, it is not essentially responsible for the occurrence of a pronounced peak in a limited mass ratio region. As mentioned in the appendix, other assumptions of deformation lead to Coulomb energy curves nearly parallel to each other. Therefore, the main feature remains the same and we may conclude that the deformation assumption is not critically related to the prediction of asymmetric fission.

(4) Deformation energy. The total deformation energy used here is nearly constant with respect to the mass ratio of splitting. Thus, it plays no essential part in the determination of asymmetric fission. Its introduction merely causes the maximum excitation energy curve to shift downward without essentially changing its shape.

The main factor involved in the calculation of relative probabilities by Eq. (45) is the level-density expression and the formula for the total density of quantum states. As the density of quantum states is a monotonically increasing function of the excitation energy, a calculation using a different expression for the density will give merely a different scale of the ordinate of the mass distribution curve. The asymmetry will remain.

In conclusion, we may say: Because the nuclear masses are smaller by a few Mev in the broad neighborhood of shell edges[43] (due to the correction terms ΔM_A and ΔZ_A), fission fragments in these regions (which happen to be in the asymmetric fission region) will have larger excitation energies. As the density of quantum states is a rapidly increasing function of the excitation energy, a small increase in excitation energy may cause a large increase in relative probability. Thus, we have a pronounced asymmetric splitting in fission.

As the explanation of asymmetric fission hinges on the result that asymmetric modes have larger excitation energies than symmetric modes, it is helpful to find direct experimental evidence supporting this result. The recent work of Fraser and Milton[44] shows that fission modes in the peak yield region have larger prompt neutron emission probabilities than symmetric fission. From the difference of prompt neutrons, it can be estimated that the excitation energy in the peak yield region is larger than that of symmetric fission by about 6 Mev. This value is about equal to our calculated difference. Radiochemical results by Coryell,[45] Tewes and James,[46] Schmitt and Sugarman,[47] and Steinberg and Glendenin[48] also indicate smaller neutron emission probability for symmetric fission.

[40] The relation between shell structure and asymmetric fission has been suggested and discussed by Mayer,[41] Meitner,[42] and later many others from different points of view.

[41] M. G. Mayer, Phys. Rev. **74**, 235 (1948).

[42] L. Meitner, Nature **165**, 561 (1950), and Arkiv Fysik **4**, 383 (1952).

[43] The nuclear mass surface is affected by nuclear shell structure in two ways: (1), A local discontinuity from nonmagic to magic nuclides of the same mass number; (2), A broad depression of the surface in the neighborhood of shell edges affecting a few nucleons on both sides of the edge. It is the latter effect that is related to asymmetric fission.

[44] J. S. Fraser and J. C. D. Milton, Phys. Rev. **93**, 818 (1954).

[45] C. D. Coryell (private communication).

[46] H. A. Tewes and R. A. James, Phys. Rev. **88**, 860 (1952).

[47] R. A. Schmitt and N. Sugarman, Phys. Rev. **89**, 1155 (1953).

[48] E. P. Steinberg and L. E. Glendenin, Phys. Rev. **95**, 431 (1954).

VII. OTHER APPLICATIONS

Other applications of the statistical theory will be discussed briefly. Preliminary results have been given in reference 39. Details will be published in the future.

a. Charge Distribution

Equation (43) gives a charge distribution curve of primary fission products which is approximately a Gaussian with a width given by Eq. (44). Typical half-width at half-maximum has been calculated to be 0.6 charge unit. The beta-decay chain lengths of the pair of primary fragments have a ratio around 1.1 for the most probable charge division. Experimental evidence seems to indicate that the width is about 0.8 or 1.0 charge unit and that the chain lengths are equal.[49]

b. Kinetic Energy Distribution

The average value of Coulomb energy given in Fig. 6 is 171.7 Mev. This may be compared with the experimental value of the average kinetic energy of a pair of fission fragments, 167.1 Mev.[50] The energy-*versus*-mass-ratio curve in Fig. 6 is nearly parallel to the experimental curve[51] and the discrepancy in the region of mass ratio 1.1 to 1.2 has been discussed.[37] Typical calculated values of the width of the kinetic energy distribution curve are 5 Mev (half-width at half-maximum). The experimental value[51] after correction for dispersion[37] is about 7 Mev.

c. Variation of Distributions with Respect to Target Nucleus

The peak in the maximum excitation energy curve is a result of the superposition of the dips of the curves in Fig. 2 and Fig. 3. When the mass number of the target nucleus changes, these dips shift apart to form a new superposition pattern. Consequently, there will be changes in peak position and width of the mass distribution curve.

d. Variation of Distributions with Respect to Incident Energy

When fission is induced by particles of high energy, Eq. (28) predicts little change in kinetic energy, a fact which has been confirmed experimentally.[3] Therefore, the excess energy must go into excitation. When the excitation energy is high, the small differences, of the order of a few Mev, between its values for different modes of fission, become less important. Therefore, at high energy, symmetric and asymmetric fission will have comparable probabilities. All rare modes of fission will become more probable. However, the most probable modes will remain to be most probable. This means that the widths of all distribution curves will be increased while the peaks of all distribution curves remain unshifted. This prediction has been corroborated by a large number of experiments.[3]

e. Prompt Neutron Distribution

The distributions of excitation energy E and deformation energy D determine the distribution of final excitation energy H. As H is the energy available for neutron emission, the distribution of prompt neutron may be derived. The most probable value of H has been calculated to be 26.5 Mev, which may be compared with the average value estimated by Brunton.[8] Brunton's value should be changed to 22.5 Mev according to the correct number of prompt neutrons emitted per fission. The distribution of prompt neutrons with respect to mass ratio of splitting has been discussed in Sec. VI.

f. Spontaneous Fission Yields

In spontaneous fission the absolute value of excitation energy will be less than that of thermal neutron fission by an amount nearly equal to the neutron binding energy. Therefore, the same differences of excitation energy among fission modes will now have a more pronounced effect on relative probability. Consequently, the rare modes will become even rarer. This prediction has been corroborated by experimental facts.[52]

g. Ternary Fission

Occasionally, an α particle is emitted in the fission process. The calculation shows that the total excitation energy will be lessened by a few Mev due to the emission of an α-particle. As a result the corresponding relative probability will be decreased by a few orders of magnitude. The observed rate of such events is one in 400 binary fission events.[53]

ACKNOWLEDGMENTS

The author wishes to express his deep gratitude to Professor Maria G. Mayer for her constant guidance and valuable suggestions. He is grateful to Professor A. Turkevich, Professor G. Wentzel, Professor M. L. Goldberger, Professor V. L. Telegdi, and Professor M. Gell-Mann for many suggestions and discussions. Valuable suggestions from Professor E. Fermi are also acknowledged. The author is indebted, for many valuable discussions and for communication of unpublished work, to Professor C. D. Coryell and Dr. A. C. Pappas (particularly beta-decay energetics), to Dr. R. B. Leachman and Dr. J. S. Fraser (particularly fission kinetic energy and fission neutrons) and to Dr. L. E.

[49] L. E. Glendenin, Office of Naval Research Report ONR–35, 1949 (unpublished).
[50] R. B. Leachman, Phys. Rev. **87**, 444 (1952).
[51] D. C. Brunton and G. L. Hanna, Can. J. Research **A28**, 190 (1950); Phys. Rev. **75**, 990 (1949). D. C. Brunton and W. B. Thompson, Can. J. Research **A28**, 498 (1950); Phys. Rev. **76**, 848 (1949).
[52] J. MacNamara and H. G. Thode, Phys. Rev. **80**, 471 (1950).
[53] K. W. Allen and J. T. Dewan, Phys. Rev. **80**, 181 (1950).

Glendenin and Dr. E. P. Steinberg (particularly charge distribution). The use of experimental data of Dr. H. E. Duckworth and Dr. D. J. Hughes before publication is gratefully acknowledged. The author also wishes to take this opportunity to thank the many people with whom he has had helpful discussions for their valuable comments and encouragement.

APPENDIX. MUTUAL COULOMB ENERGY OF TWO DEFORMED FRAGMENTS IN CONTACT

The mutual Coulomb energy between two deformed fragments, like the ones in Fig. 5, will be calculated approximately.

The potential at a point P due to a uniform charge sphere Ze is Ze/D, where D is the distance from P to the center of the sphere O. Let the direction OP be chosen as the polar axis and assume the sphere to be deformed according to the following formula:

$$r=r_0[1+\alpha_3 P_3(\cos\theta)].$$

When α_3 is small compared to unity, the potential at P will be increased by an amount δV given by

$$\delta V=\frac{Ze}{(4\pi/3)r_0^3}\int\int_S \frac{r_0\alpha_3 P_3(\cos\theta)dS}{(D^2+r_0^2-2Dr_0\cos\theta)^{\frac{1}{2}}}$$

$$=\frac{3}{7}\alpha_3\left(\frac{r_0}{D}\right)^3\frac{Ze}{D}.$$

This accounts for the linear term of α_3 and we shall limit ourself to this approximation. The effect of deformation on the potential at P is the same as that due to a shift of the "charge center" of the sphere from O to O' with the distance between O and O' equal to $(3/7)r_0\alpha_3(r_0/D)^2$. The mutual Coulomb energy of the two deformed spheres in Fig. 5 may be expressed approximately as follows:

$$\begin{aligned}C&=Z_1Z_2e^2/[O_1',O_2']\\&=Z_1Z_2e^2/\{[O_1,O_2]-[O_1,O_1']-[O_2,O_2']\}\\&=Z_1Z_2e^2\Big/\left\{[r_{01}(1+\alpha_{31})+r_{02}(1+\alpha_{32})]\right.\\&\qquad\left.-\frac{3}{7}\alpha_{31}r_{01}\left(\frac{r_{01}}{[O_2',O_1]}\right)^2-\frac{3}{7}\alpha_{32}r_{02}\left(\frac{r_{02}}{[O_1',O_2]}\right)^2\right\}.\end{aligned}$$

$r_{01}/[O_2',O_1]$ and $r_{02}/[O_1',O_2]$ vary slowly with respect to α_{31} and α_{32}, and they appear in small terms in the denominator. Thus we may regard them as constants. Their values may be determined by successive approximation. Both of them are approximately 0.4 for α's in the neighborhood of their most probable values. By numerical substitution of this value, the above equation reduces to Eq. (16) of Sec. IV.

The above method may be used to calculate the mutual Coulomb energy of two fragments deformed according to any Legendre polynomial provided that the deformation is small. The deformation energies of these fragments (up to the P_5 term) may also be obtained from the expression by Present and Knipp.[36] Thus the maximizing procedure of Sec. IV may be repeated to obtain the most probable values of mutual Coulomb energy and deformation energies. The results[37] of calculation based on several alternative assumptions of deformation show that: the relative variation of the most probable Coulomb energy C with mass ratio is nearly the same in all cases but the absolute value of C depends on deformation assumption sensitively; the most probable deformation energies D_1 and D_2 are nearly constant with respect to mass number in all cases and their absolute values vary within a few Mev for different assumptions of deformation.

For the relative probabilities of fission modes, the relative variation of C and D from one fission mode to another is important, and this is insensitive to the assumption to the type of deformation. Thus our assumption that fragments are deformed according to $P_3(\cos\theta)$ only, though an oversimplified one, is sufficient for the purpose of comparing relative probabilities.